Clays Clay Miner., Vol. 71, No. 4:430–447, 2023
https://doi.org/10.1007/s42860-023-00246-4

ORIGINAL PAPER

Organic Exfoliation of Hydrophilic Bentonite using Aliquat 336 and Isobutyl(Trimethoxy)Silane to Enhance its Activity Toward pH-Dependent Adsorption of Epigallocatechin Gallate

Alimpia Borah · Akhil Ranjan Borah · Monti Gogoi · Rajiv Goswami · Swapnali Hazarika

Accepted: 26 June 2023 / Published online: 30 August 2023

Abstract The most potent and significant polyphenolic molecule from tea catechins is epigallocatechin gallate (EGCG); it has potential anti-cancer and anti-inflammatory properties. Methods are needed to mitigate its presence in the environment and protect humans from exposure. The objective of the present study was to investigate a functionalized, low-cost clay mineral as an adsorbent for the tea polyphenol EGCG. Hydrophilic bentonite (Bn) was functionalized using Aliquat 336 (A336) and isobutyl(trimethoxy)silane (IBTS). The degree of clay functionalization depended on the extent of introduction of alkyl linkages between the superimposed clay layers. Results revealed that Aliquat 336 functionalized clay (A336-Bn) exhibited maximum thermal stability at 500°C and it is a promising adsorbent for ECGC with a maximum adsorption capacity of 196.26 mg/g at equilibrium. Experimental data were analyzed using pseudo-first order and pseudo-second order models. Adsorption isotherms were interpreted from the Freundlich adsorption isotherm.

A. Borah · A. R. Borah · M. Gogoi · R. Goswami · S. Hazarika (✉)
Chemical Engineering Group and Centre for Petroleum Research, CSIR-North East Institute of Science and Technology, Jorhat 785006, Assam, India
e-mail: shrrljt@yahoo.com

A. Borah · M. Gogoi · R. Goswami · S. Hazarika
Academy of Scientific and Innovative Research (AcSIR), Ghaziabad 201002, India

Keywords Adsorption · Epigallocatechin gallate · Hydrophilic bentonite · Silane coupling agent · Surfactant

Introduction

Bentonite (Bn) is a naturally occurring mineral ore that contains montmorillonite (Mnt), an aluminosilicate belonging to the smectite group with a chemical composition that includes alkali metal ions (Anastácio et al., 2008; Bai et al., 2019; Bergaya & Lagaly, 2006). When modified with an organic surfactant through cation exchange in the Mnt interlayers, small amounts of Mnt can be exfoliated to form clay-polymer nanocomposites (Beltrán et al., 2014). These materials have received a great deal of attention because of the beneficial properties imparted to the polymers by the presence of the clay mineral (Manias et al., 2001). Quaternary ammonium cations are among the most common of such organic modifiers, but silane coupling reagents have also been exploited to further propagate the organic intercalation process specific to the use of silane compounds (Raji et al., 2018). Functionalized clays have also been exploited for many other purposes, including the adsorption and/or sequestration of an abundant array of hydrophobic compounds (Park et al., 2011).

In general, quaternary ammonium compounds contain hydrophobic alkyl chains that are attached to the positively charged nitrogen atom (Komoriet al., 1999). The surfactants can be used for the

development of hybrid polymeric composites (Li et al., 2018; Moreno et al., 2006). Cationic surfactants can be used for the surface modification of hydrophilic aluminosilicates and they can also be used as adsorbents in various adsorption processes (Asefi et al., 2009, 2010).

The physicochemical properties of clay minerals can be changed by exchange with quaternary ammonium cations to increase their reactivity toward a wide array of organic compounds (Terzic et al., 2017; Zhou et al., 2015). The reaction of quaternary nitrogen is increased by the polarization of the basal oxygen atoms that are embedded at the clay surface (Zumsteg et al., 2014). The formation of functionalized clay can be carried out by intercalation which involves cation exchange capacity, concentration gradient of surfactants, and diminishing surface area (Guo et al., 2018). By virtue of its high Mnt content, bentonite has a much larger cation exchange capacity and greater hydrophilicity than kaolinite (Kln).

Aliquat 336 is a cationic surfactant with a long hydrophobic alkyl chain (Kozak & Domka, 2004), and it also has phase-transfer capacity in clay modification. The silane coupling agent isobutyl trimethoxy silane is the stable intermediate in epoxy based encapsulants (Leung et al., 2001). The hydrolyzable parts (alkyl chain) of silane coupling agents have significant reactive affinity with the silanol group of mineral surfaces. The functionalized clays have been chosen as an effective means of removing hazardous metals from the environment (Zhang et al., 2015). The large surface area of surfactant-loaded functionalized clay leads to a highly reactive interface with polymer matrices. Moreover, the hydrophobicity which occurs because of intercalation of the surfactants into the clay mineral layers offers functionality to the clays for various applications (He et al., 2006).

Functionalized clay nanocomposites have various applications in environmental protection through the adsorption of chemicals such as 2,4-dichlorophenol using functionalized clay/aquifer material mixtures, Cu(II), and dyes, etc. (Mahmoodi & Arami, 2009; Oveisi et al., 2019; Paiva et al., 2008; Pernyeszi et al., 2006; Xie et al., 2018). Clay mineral interlayers can be transformed from being hydrophillic to hydrophobic by exchanging the natural inorganic cations with surfactant cations (Düşkünkorur et al., 2015; Tonle et al., 2015). Functionalized clay minerals serve as efficient catalysts for the ring-opening polymerization reaction of the lipase enzyme (Ozturk et al. 2016). In addition to this, functionalized clays are most effective in removing phenolic compounds from organic-solution mixtures (Moshe & Rytwo, 2018; Li et al., 2019).

Previous studies have reported the use of functionalized clay for the adsorption of dyes or other contaminants. The use of hexadecyltrimethylammonium (HDTMA) chloride-modified bentonite as an adsorbent for basic dyes such as methylene blue, crystal violet, and rhodamine B was studied by Anirudhan & Ramachandran (2015) who achieved a maximum adsorption of methylene blue of 399.74 μmol/g. The surfactant functionalization of clay minerals and its use for the adsorption of p-chlorophenol and p-nitrophenol was studied by Park et al. (2013); the amounts adsorbed were reported as 14.286 and 12.870 mg/g, respectively. The sorption of benzene and metals by functionalized clays (HDTMA-bentonite and BTEA-bentonite) was studied by Oyanedel-Craver et al. (2007). Some researchers suggested the use of functionalized clays for the adsorption of non-ionic organic compounds (NOC) (Oyanedel-Craver et al., 2007; Park et al., 2013).

The advantages of functionalized clays as adsorbents include the following: (1) regeneration can be quick and easy; (2) desorption is chemically simple; (3) non-toxic by-products are produced; (4) they can work at low temperatures; (5) their large adsorption capacity for organic compounds such as EGCG reduces the amount that must be used as adsorbent and helps to minimize disposal volumes (Mahmoodi et al., 2010a); and (6) they are cheap.

The main goal of the current study was to create reactive platforms within the clay layers by functionalizing the bentonite using Aliquat 336 or isobutyl(trimethoxy) silane (IBTS) and then comparing their characteristics. A further objective was to demonstrate the effect of alkyl linkage on the clay functionalization process and to present a novel modification method for clay-based material for the purpose of polyphenol separation.

Experimental

Materials

Hydrophilic bentonite (≤25 μm) and cationic surfactant Aliquat 336 (>97% purity) were purchased from Sigma Aldrich (Bangalore, India). The cation

https://doi.org/10.1007/s42860-023-00246-4 Published online by Cambridge University Press

exchange capacity of this clay is 92 meq/100 g. The high-purity isobutyl(trimethoxy)silane [$(CH_3)_2CHCH_2Si(OCH_3)_3$, 97%] coupling reagent was purchased from Merck (Bangalore, India). The polyphenol epigallocatechin gallate ($C_{22}H_{18}O_{11}$, > 98%, HPLC) was procured from Sigma Aldrich (Bangalore, India) and used in the adsorption study. The distilled water used throughout the experiments was obtained from the Milli-Q water system. The commercially available standard Oakton pH buffer solution was purchased from Cole-Parmer (Mumbai, India). The composition of the standard acidic buffer solution was a mixture of deionized water (H_2O) and potassium hydrogen phthalate ($C_8H_5O_4K$), whereas the basic buffer standard had a composition of deionized water (H_2O) and sodium phosphate (Na_2HPO_4).

Purification of the Bentonite Clay

In order to separate the Mnt from bentonite, the particles were centrifuged at 1500 rpm (378 × *g*) for 15 min, followed by ultrasonic treatment to separate montmorillonite fractions from raw bentonite. 5 g of raw bentonite was dispersed in 100 mL of deionized water and sonicated for 30 min. The suspension was then centrifuged at 1500 rpm (378 × *g*) for 15 min to settle the solid particles. The upper fraction of the dispersed material was collected and poured into a beaker for evaporation of water under oven drying at 150ºC which was complete after 12 h. Acid treatment of the raw bentonite was carried out to remove iron oxide and carbonate adsorbed on the clay. 5 g of raw bentonite was treated with 0.05% of acetic acid solution at pH 5 by adding sodium acetate. The mixture was further centrifuged at 1500 rpm for 15 min to collect the clay.

Other organic matter in the Bn clay was removed by adding 0.05 mol L^{-1} sodium acetate and 85 mL of H_2O_2. The centrifugation process was done at 1500 rpm (378×*g*) for 10 min to separate the solid phase. The purified bentonite was washed with sodium chloride to obtain sodium-saturated bentonite.

Preparation of the Functionalized Clay (Modified Bentonite)

For the functionalization of the clay, 1 g of acid-activated raw bentonite was added to a mixture of 20% distilled water and 80% methanol, which was stirred continuously at 75°C. The clay dispersion was sonicated for 30 min at 25°C to disperse the stacked layers. After the dispersion, the solution was separated into two parts;1 mL/g of Aliquat 336 (organic modifier) was added to one part, 1 mL of isobutyl(trimethoxy)silane was added to the other. Afterward, both mixtures were stirred for 4 h, then centrifuged at 1500 rpm (378 × *g*) for 5 min so that separation of the solid and liquid phases was achieved. The modified clay was dried in an oven at 60ºC for 24 h. The dried solids were ground for further use.

Characterization of Raw, Purified, and Functionalized Clay

The structural differentiation between raw clay, and functionalized clay was determined using various experimental techniques. The FTIR spectra were recorded over the range 400 to 4000 cm^{-1} using a Perkin-Elmer Spectrum 100 spectrophotometer (Kenilworth, New Jersey, USA). A Zeiss Sigma Field-Emission Scanning Electron Microscope (Oberkochen, Germany) was used to analyze the surface morphology and energy dispersive X-ray analysis (EDX) to determine the elements present in the raw and purified bentonite. The interlayer morphology of the clays was characterized by high-resolution transmission electron microscopy (HRTEM) using a JEM 210 Plus electron microscope (JEOL, Tokyo, Japan). The interlayer spacing of the clay layers was also determined by X-ray diffraction using a Rigaku ULTIMA-IV instrument (Tokyo, Japan). The elemental compositions of the functionalized clay were analysed using an X-ray photoelectron spectrometer, ESCALAB Xi + (Thermo Fisher Scientific, East Grinstead, UK). A chemisorption and physisorption instrument (Anton Paar, Ostfildern-Scharnhausen, Germany) was used to determine the BET (Brunauer Emmett Teller) surface area of the sample. In the BET adsorption experiment, the volume of gas adsorbed on the surface was measured at discrete pressures over the relative equilibrium adsorption pressure (P/P_0) range of 0.075–1.0, where P and P_0 are the absolute equilibrium pressure and condensation pressure of nitrogen, respectively.

https://doi.org/10.1007/s42860-023-00246-4 Published online by Cambridge University Press

Adsorption Experiment

A batch experiment was performed to investigate the adsorption capacity of raw bentonite and its functionalized form for adsorption of EGCG from its aqueous solution. The initial concentration of the EGCG solution was taken as 1 mg/L. The amount of adsorbent used for every adsorption experiment was 5 mg. The adsorbent was dispersed in an aqueous solution of EGCG under continuous agitation for 12 h. After shaking properly, the mixture was centrifuged for 10 min, and the supernatant was collected and analyzed using a Spectroquant® Prove 600 UV/Vis spectrophotometer (Darmstadt, Germany). The pH-dependent adsorption of raw bentonite and functionalized clays were determined by evaluating the amount of EGCG adsorbed under five different pH values (3, 5, 7.5, 8, and 9). The aqueous solution of EGCG was added to five different conical flasks to each of which one of the pH buffer solutions was added. For each solution, 0.1 g of functionalized clay was added and the mixture was stirred at 500 rpm for 6 h. The supernatant of each solution was collected and analyzed using a UV–Vis spectrophotometer (Spectroquant® Prove 600 UV/Vis spectrophotometer (Darmstadt, Germany)).

To test and compare the adsorption performances of the functionalized clays, the adsorption capacity (q_e, mg/g) of pure and functionalized clays for polyphenol was calculated using Eq. (1)

$$q_e = \frac{C_0 - C_e}{m} \times V \tag{1}$$

where C_0 (mg/L) and C_e (mg/L) are the concentrations of the polyphenol in solution before and after adsorption equilibrium, V (L) is the volume of the polyphenol solution, and m (g) is the mass of the adsorbent used.

The removal efficiency ($R\%$) of the polyphenol was calculated by

$$R\% = \frac{C_0 - C_t}{C_0} \times 100 \tag{2}$$

where C_t (mg/L) is the concentration of the solution obtained at various time intervals.

The adsorption kinetics (Mahmoodi et al., 2018) of EGCG onto functionalized clay can be studied using pseudo-first order and pseudo-second order kinetics models.

Pseudo-First Order Model

This model was used to express the rate of adsorption of adsorbate from a liquid phase and is known as the Lagergren rate equation, given by Mahmoodi et al. (2018):

$$\frac{dq}{dt} = \mathrm{k}_1(q_e - q_t) \tag{3}$$

where q_e and q_t (mg·g^{-1}) are the adsorption capacities at equilibrium and at time t, respectively; k_1 (min^{-1}) is the rate constant. Integrating Eq. 3,

$$\log\left(q_e - q_t\right) = \log q_e - k_1 t/(2.303) \tag{4}$$

The adsorption rate constant (k_1) is determined from the plot of $\log(q_e - q_t)$ vs. t.

Pseudo-Second Order Model

In this model, the rate of adsorption is given as (Mahmoodi et al. 2018):

$$\frac{dq}{dt} = \mathrm{k}2(q_e - q_t)2 \tag{5}$$

where k_2 (g mg^{-1} min^{-1}) is the rate constant for the pseudo-second order adsorption reaction.

Integrating this for the boundary conditions $t = 0$ to $t = t$ and $q_t = 0$ to $q_t = q_t$, gives

$$t/q_t = 1/k^2 qe2 + 1/q_{et} \tag{6}$$

The values of q_e and k_2 can be calculated using Eq. 6.

Equilibrium Study

Equilibrium adsorption isotherms were measured by performing the experiment using 0.021 g of adsorbent in 250 mL of aqueous alcohol solution. The equilibrium time for adsorption isotherms was 300 min as confirmed by kinetic data. Adsorption data were modeled using the Langmuir and Freundlich equations.

The Freundlich isotherm is typically used to model energetically heterogeneous surfaces, using the expression:

https://doi.org/10.1007/s42860-023-00246-4 Published online by Cambridge University Press

$$q_e = K_F C_e^{1/n} \quad (7)$$

where K_F is the Freundlich constant (mg g^{-1}), n is the adsorption intensity, C_e is the equilibrium concentration of the adsorbate (mg L^{-1}), and q_e is the amount of EGCG adsorbed per gram of the adsorbent at equilibrium (mg g^{-1}).

The linear form is

$$\log q_e = \log K_F + 1/n \log(C_e) \quad (8)$$

The Langmuir hypothesis states that, once a saturation point is achieved, no further adsorption can occur. At this time, the saturation monolayer is represented by the following expression:

$$q_e = (q_L K_L C_e)/(1 + K_L C_e) \quad (9)$$

where, q_e (mg g^{-1}) is the equilibrium amount of adsorbate, C_e (mg L^{-1}) is the equilibrium concentration of adsorbate, q_L (mg g^{-1}) and K_L are the Langmuir constants for monolayer adsorption capacity and energy of adsorption, respectively.

Desorption and Regeneration Studies

The desorption and regeneration study of the adsorption process was carried out to determine the nature of the adsorbate–adsorbent interaction (Mahmoodi et al. 2010c). In this process, the functionalized clay was recovered by the desorption of EGCG using dilute NaOH. The regenerated functionalized clay was again tested for further adsorption of EGCG. Both the adsorption and desorption procedures were done four times.

Results and Discussion

Determination of Functional Groups

The vibrational frequencies of the various moieties in the clay layers were determined by FTIR spectroscopy (Borah et al. 2022). Shifts in vibrational frequencies differentiated the raw, purified, and functionalized clays (Fig. 1a-d). The peak at 1015 cm^{-1} was present in all clay samples and indicated the presence of Si–O–Si stretching vibrations. The low intensity of this peak in the purified clay reflected the decrease in SiO_2 content (Fig. 1b). The band at 3523 cm^{-1}in all spectra was due to structural O–H stretching. The peak at 3170 cm^{-1}(Fig. 1c) was due to $–CH_2$ vibrations. The broadening of this peak was due to intercalation of the alkyl-chain into the clay interlayer space in the case of the surfactant

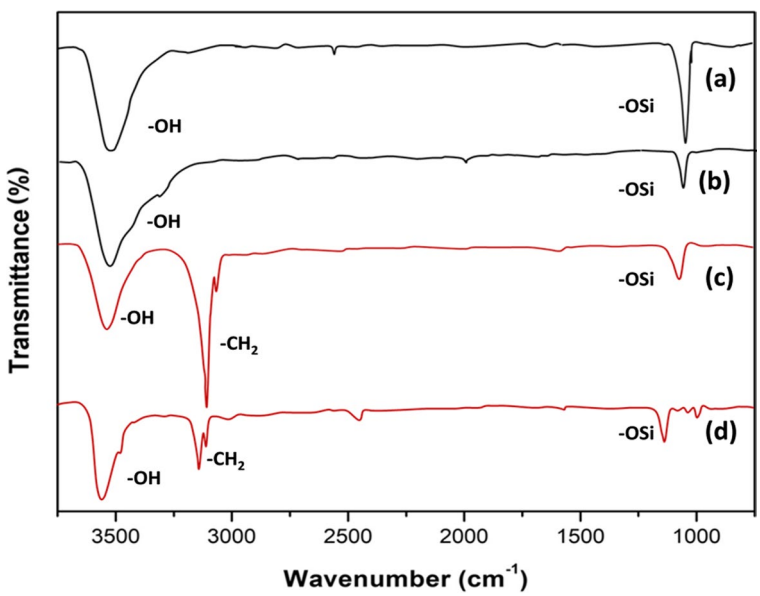

Fig. 1 FTIR spectra of **a** raw bentonite, **b** purified bentonite, **c** A336-Bn, and **d** IBTS-Bn

https://doi.org/10.1007/s42860-023-00246-4 Published online by Cambridge University Press

functionalized clays. In Fig. 1d, a low-intensity peak at 3170 cm^{-1} was observed which was perhaps due to the intercalation of isobutyl linkage in the clay layer. In Fig. 1c two peaks were obtained at 3170 cm^{-1} and 3050 cm^{-1} due to the presence of the long alkyl chain of Aliquat 336 in the functionalized clay. More exfoliation of clay layers occurred in A336-Bn compared to IBTS-Bn.

Determination of the XRD Pattern

X-ray diffraction patterns of the raw, purified, and functionalized clays (Fig. 2) showed peaks at 20.5, 28.3, 35.8, and 54.7°2θ due to the presence of (110), (210), (124), and (144) planes, respectively. These XRD patterns are in good agreement with the standard JCPDS file (01–008-0891) (Ouellet-Plamondon et al., 2014). Here, the diffraction intensities differed in raw and functionalized clays. The raw clay contained feldspar (Fsp), quartz (Qz), and cristobalite (Crs) at 32.5°, 56.1°, and 40.5°2θ, respectively. In the case of surfactant-functionalized clay, the intensity of the diffraction peak increased due to the intercalation of long alkyl chains within the clay layers.

The low intensity of the d_{110} reflection was observed in silane coupling with the clay because of the methyl fragment (Abeywardena et al. 2017). The d spacings were 1.55, 1.52, 1.40, and 1.38 nm for the surfactant-modified, silane-modified, purified, and raw bentonites, respectively. The lower angle in the modified clay compared to raw bentonite indicated the widening of a peak with an increase in interlayer spacing. The elongation of the silane-group hydrophobic fragments was attributed to the comparatively weaker intercalation within the clay-polymer skeleton (Avella et al. 2005). The stacked layers of the clay were more exfoliated in the case of the surfactant functionalized clay due to the longer alkyl chain. The intensity of the corresponding diffraction peaks increased therefore (Fig. 2c).

Elemental Analysis

The use of XPS is a prerequisite for analyzing the elements involved in intermolecular attractions which leads to different binding energies due to factors such as electronegativity, electron affinity, and polarizability. Survey XPS spectra of the raw, surfactant functionalized, and silane-coupled clay (Fig. 3) showed in the raw clay (Fig. 3E) binding energies for Si, C, and O at 102, 270, and 532 eV, respectively. The high-resolution XPS scan of the C1s peak for the raw clay showed a peak at 284 eV which confirms the presence of the C–C bond (Fig. 3A.1). Further, for the O1s high-resolution scan, two distinct peaks were obtained at binding energies of 531 and 532 eV which correspond

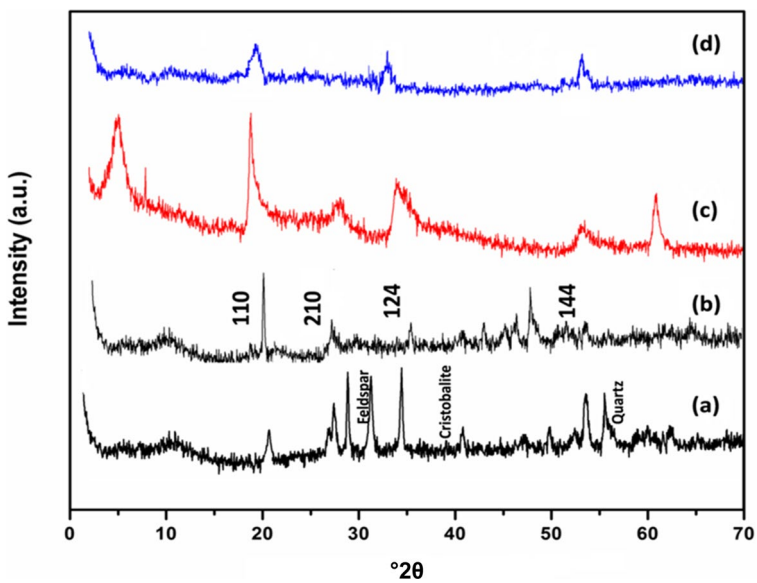

Fig. 2 Powder XRD patterns of **a** raw bentonite, **b** purified bentonite, **c** A336-Bn, and **d** IBTS-Bn

https://doi.org/10.1007/s42860-023-00246-4 Published online by Cambridge University Press

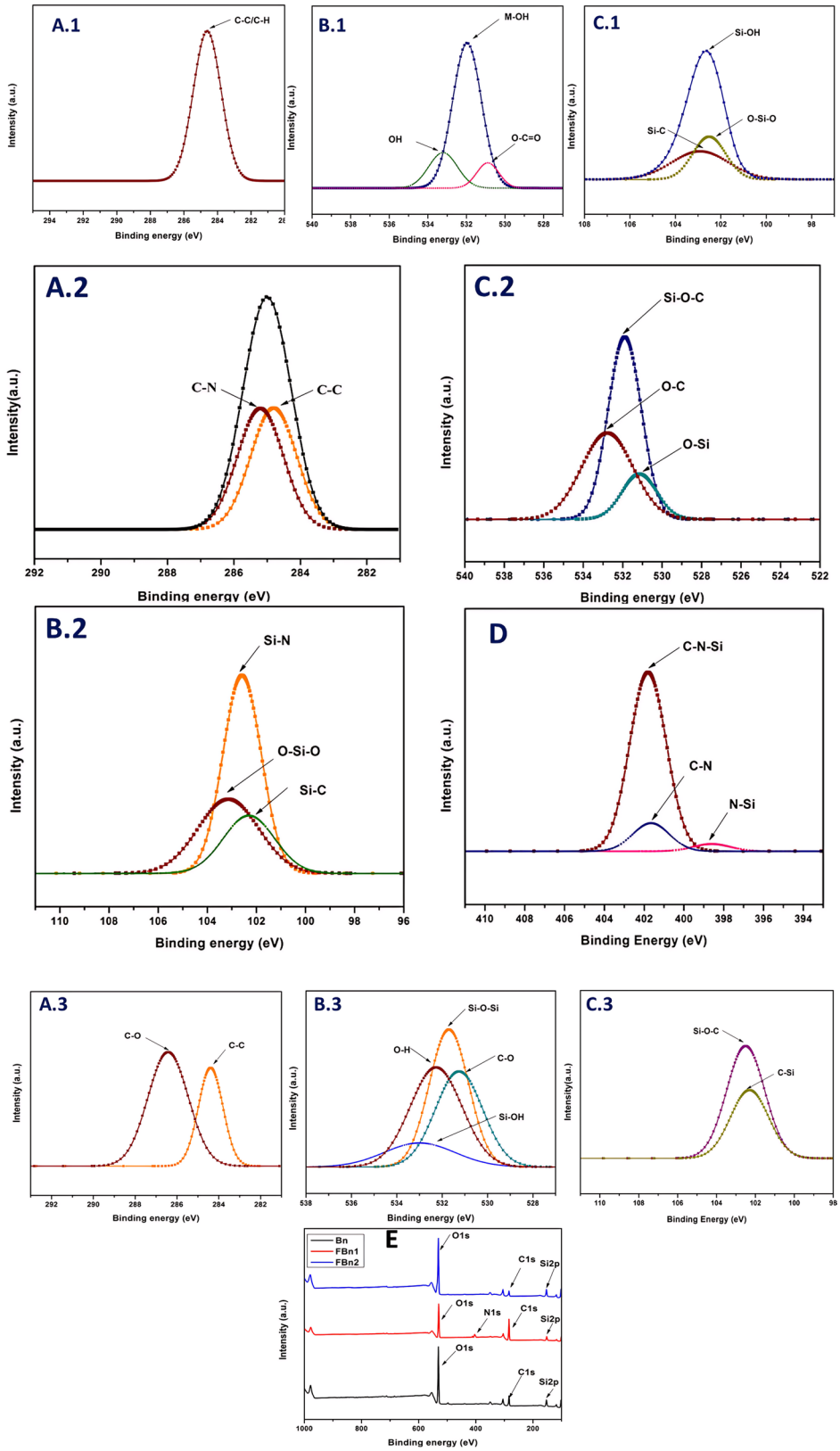

Fig. 3 High-resolution XPS spectra of C1s (A.1, A.2, A.3), O1s (B.1, B.2, B.3), Si2p (C.1, C.2, C.3), and N1s (D), and survey scans (E) of raw bentonite, A336-Bn, and IBTS-Bn

https://doi.org/10.1007/s42860-023-00246-4 Published online by Cambridge University Press

to metal carbonate and metal hydroxide, respectively (Fig. 3B.1). In addition to this, the high-resolution scan of Si resulted in three peaks at binding energies of 102.5, 103, and 103.3 eV which correspond to O–Si–O, Si–OH, and Si–C, respectively (Fig. 3C.1).

The XPS survey spectra of surfactant functionalized bentonite (Fig. 3E) indicated the presence of Si, C, N, and O at binding energies of 102, 270, 401, and 532 eV, respectively. A high-resolution C1s spectrum showed binding energies at 284.7 and 285.2 eV for C–C and C–N, respectively, as shown in Fig. 3A.2. Furthermore, from an N1s high-resolution scan, three peaks were obtained at 399, 401, and 402 eV, for N–Si, C–N, and C–N–Si, respectively (Fig. 3D). The O1s high-resolution scan gave three peaks at binding energies of 531, 533, and 532 eV, which correspond to O–Si, O–C, and Si–O–C (Fig. 3B.2). In addition to this, the high-resolution scan of Si revealed in three peaks, at binding energies of 102, 102.5, and 103 eV, which corresponded to Si–C, Si–N, and O–Si–O, respectively (Fig. 3C.2).

The survey spectra of silane-coupled bentonite (Fig. 3E) indicated the presence of Si, C, and O at binding energies of 102, 270, and 532 eV, respectively. The high-resolution XPS survey scan of C1s showed clearly two peaks at binding energies of 284.5 and 287 eV, which were attributed to the C–C and C–O bonds (Fig. 3A.3). Further, for O1s, in the high-resolution scan, four peaks were obtained at binding energies of 531, 532, 532.5, and 533.5 eV due to C–O, Si–O–Si, O–H, and Si–OH, respectively (Fig. 3B.3). The high-resolution scan of Si resulted in two peaks at binding energies of 102.5 and 103 eV corresponding to C–Si and Si–O, respectively, (Fig. 3C.3).

Determination of Thermal Stability

The thermal stability of the bentonite and functionalized clays were studied before and after adsorption by thermogravimetric analysis (TGA) (Fig. 4A and B). The first step in the mass loss from the raw clay (Fig. 4A(a)) below 100°C was due to the desorption of water molecules from the bentonite. In the second step (Fig. 4A(b)), the mass loss occurred at ~ 130–150°C due to the dehydration of clay interlayers. degradation of aluminosilicate interlayers. The third mass-loss at ~ 600–800°C was due to the dehydroxylation of the aluminosilicate.

The second mass loss step for surfactant-functionalized clay was observed at ~200ºC as shown in Fig. 4A(c) which revealed the dehydration of the hydrated sphere surrounding metal cations (Naranjo et al., 2013). The third weight loss was attributed to the removal of organic filler as reported by Tian et al. 2017. Curve (c) in Fig. 4A did not show the distinct peak of thermal decomposition of the surfactant fraction.

The thermal stability of surfactant functionalized clay was observed up to 550°C after adsorption, whereas before adsorption, thermal stability was observed at 600°C.

The derivative thermogravimetric (DTG) curve of the bentonite and functionalized clays (Fig. 4C) revealed four mass-loss steps in the surfactant-functionalized (Fig. 4C(b)) sample but only two in the silane-functionalized (Fig. 4C(c)) sample. The first one occurred at ~70ºC in both, due to the desorbed water. The silane-functionalized samples experienced a second mass loss at higher temperature (~430°C) than the other clays. This is attributed to the chemical change that occurred within the clay layers due to the silane-grafting ability of isobutyl(trimethoxy)silane with the hydroxyl group at the edges of the tetrahedral sheet, which stabilized the functionalized clay structure.

Surface Morphology

Surface morphology of raw and functionalized clays were analysed by SEM (Fig. 5a-d) which showed prominently stacked layers in the raw bentonite (Fig. 5a,b). In the case of functionalized clays, distinct exfoliation of stacked clay layers was observed and it was even more evident in the surfactant-modified clays (Fig. 5b,c). SEM–EDX analysis of the clays gave the picture of the elements present in the clays as shown in Table 1.

The morphology of raw and functionalized clays was also analysed by TEM (Fig. 6a–c) and, in the case of raw clay (Fig. 6a), revealed a lamellar arrangement of the clay layers, whereas in case of functionalized clays, delamination of clay structures was observed (Fig. 6b,c). The delamination occurred due to the incorporation of alkyl chains present in the surfactant and silane. The findings also revealed smooth surfaces in the case of functionalized clays (Pandey & De 2018; Zampori et al., 2010).

https://doi.org/10.1007/s42860-023-00246-4 Published online by Cambridge University Press

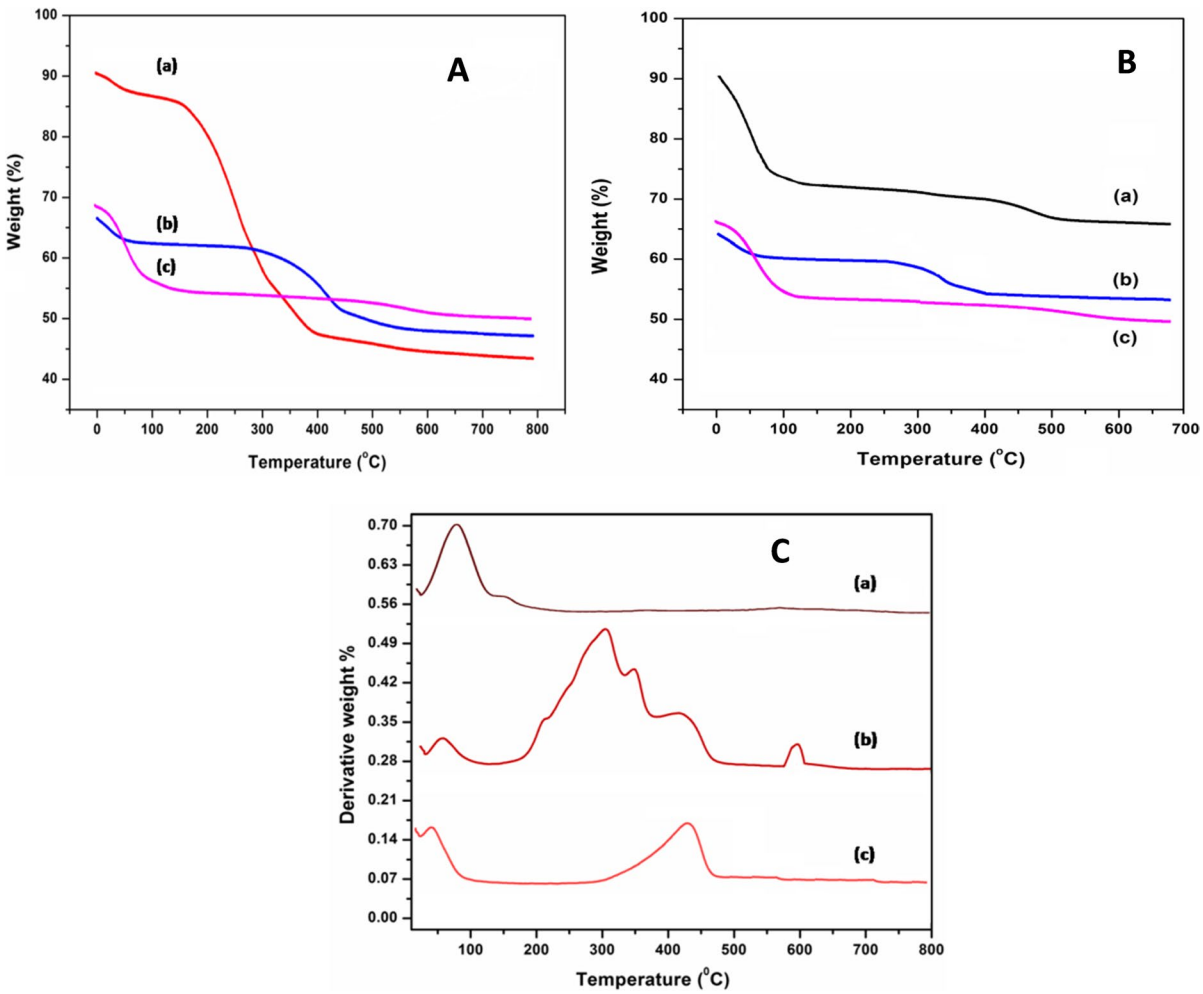

Fig. 4 TGA representation **A** before adsorption, **B** after adsorption, and **C** derivative TG curves of (a) raw bentonite, (b) A336-Bn, and (c) IBTS-Bn

Surface Roughness

Atomic force microscopy (AFM) analysis was used to assess the dispersion of surfactant or silane in the clay matrix and the external surface roughness (Fig. 7). The rougher the surface, the greater the dispersion of long hydrophobic chains within the clay matrices. The non-homogeneous dispersion with a cluster of clay on the outer surface of the clay composite was also observed. The surface roughness of the raw bentonite and functionalized clays was determined by AFM characterization in tapping mode. The average roughness (R_a) of raw bentonite, surfactant- and silane-functionalized bentonite was 11.782, 51.087, and 12.253 nm, respectively. Upon functionalization, the roughness of the clay increased, and this improvement also increased the surface area and, thus, the potential for more efficient mass transfer.

Surface Area

Surface area analysis of the clays based on N_2 adsorption experiments (Fig. 8) found the BET surface area to be 43.374 $m^2\ g^{-1}$ for the raw bentonite. After functionalization, the surface area decreased to 13.14 $m^2\ g^{-1}$ for surfactant-functionalized clay and 16.42 $m^2\ g^{-1}$ for silane-functionalized clay.

In the surfactant-functionalized bentonite, the long alkyl chains were intercalated between the superimposed clay layers and increased reactive

https://doi.org/10.1007/s42860-023-00246-4 Published online by Cambridge University Press

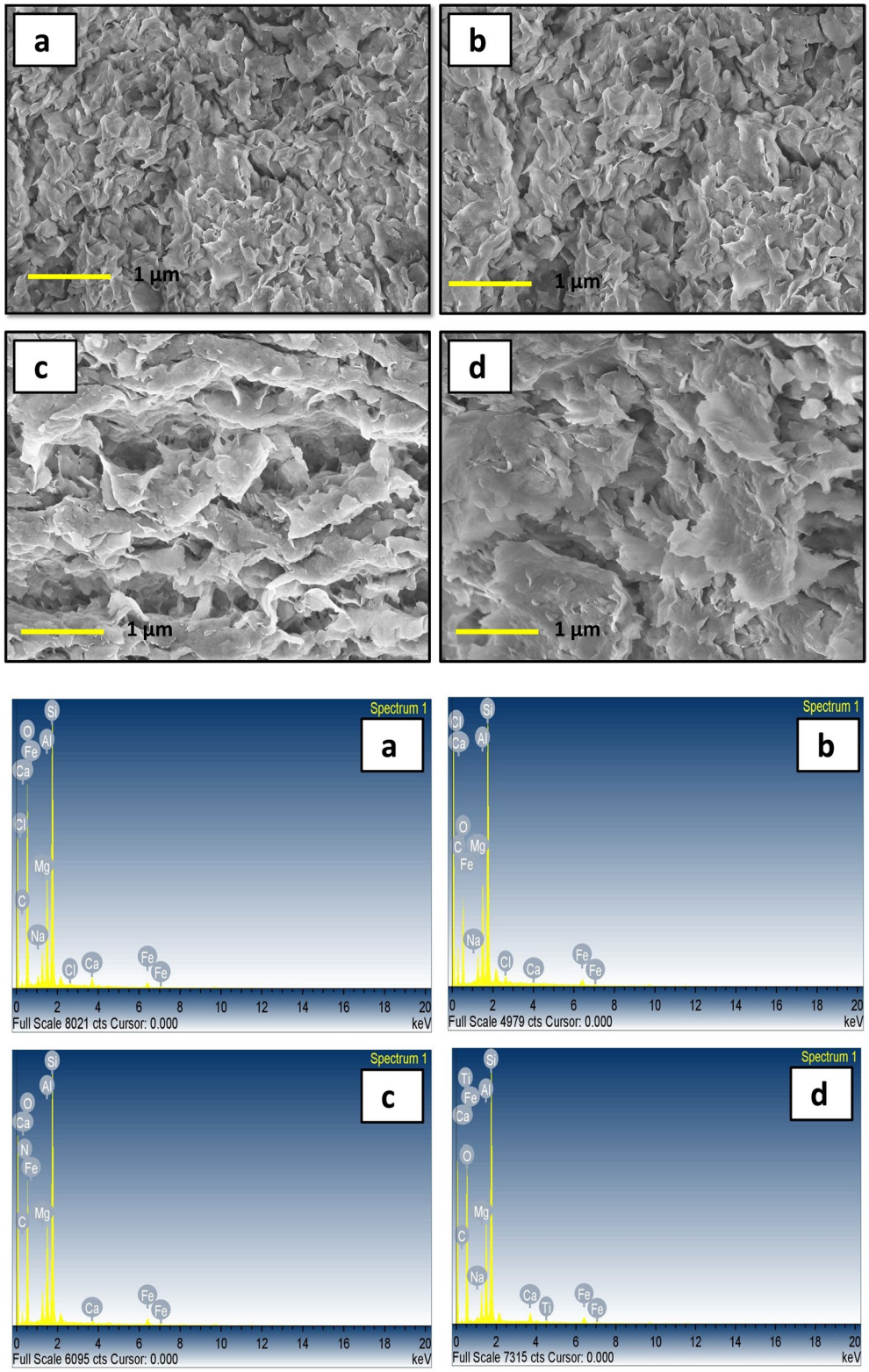

Fig. 5 SEM and EDX images of **a** raw bentonite, **b** purified bentonite, **c** A336-Bn, and **d** IBTS-Bn

https://doi.org/10.1007/s42860-023-00246-4 Published online by Cambridge University Press

Table 1 Amounts of various elements present in the raw and purified clays, by EDX analysis

Serial Number	Element %	Raw bentonite	Purified bentonite
1	C	30.08	5.20
2	O	54.86	34.69
3	Na	0.09	1.10
4	Mg	1.71	3.01
5	Al	5.56	8.13
6	Si	24.58	17.60
7	Ca	1.17	0.09
8	Fe	1.76	1.53

sites over the clay surface for adsorption. Moreover, in the case of silane-functionalized clay, the isobutyl chain had less intercalation due to the shorter hydrophobic alkyl chain and fewer pores occupied on the clay surface. This could increase the BET surface area. The intercalation of surfactant could obstruct the clay interlayer space and be arranged as a monolayer over the outer surfaces by occupying the pores in the clay particles. This could explain why the BET surface area decreased with an increased degree of modification over the clay surface and increased surface roughness (Fig. 9).

Adsorption Study

Adsorption of EGCG was studied on raw bentonite, surfactant-functionalized bentonite, and silane-coupled bentonite and the results are shown in Fig. 9. The EGCG molecules were distributed in a relatively dispersed condition, and functionalized clay quickly adsorbed it due to the interaction through hydrogen bonding. At equilibrium, the amount adsorbed was obtained as 10.7 mg/g for raw clay, 196.26 mg/g for surfactant-functionalized clay, and 140 mg/g for silane-functionalized clay. With increases in concentration of

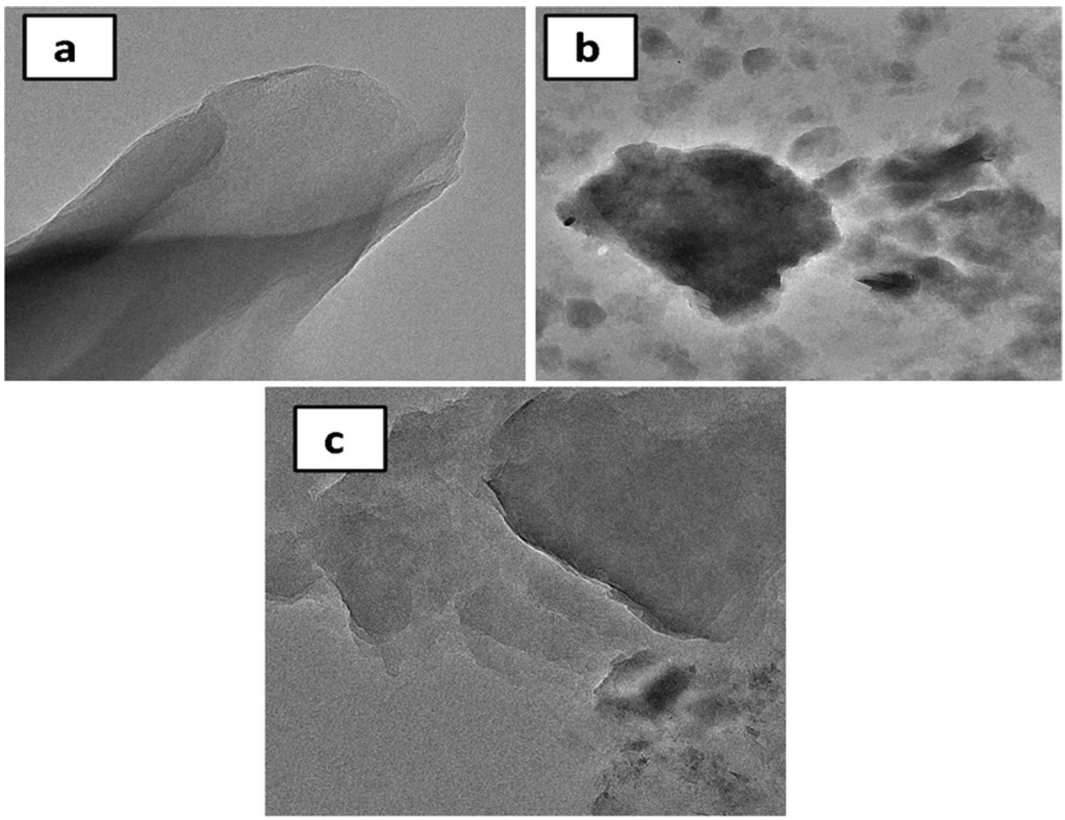

Fig. 6 TEM images of **a** raw bentonite, **b** A336-Bn, and **c** IBTS-Bn

https://doi.org/10.1007/s42860-023-00246-4 Published online by Cambridge University Press

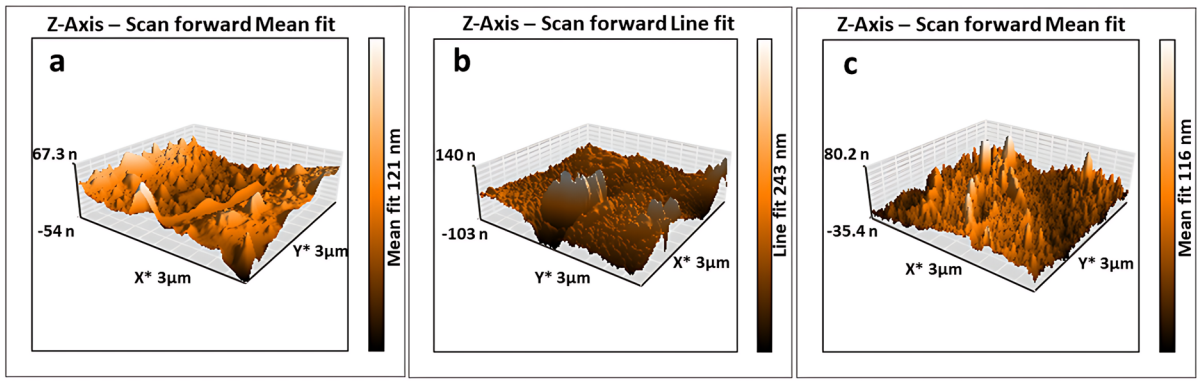

Fig. 7 AFM images of **a** raw bentonite, **b** A336-Bn, and **c** IBTS-Bn

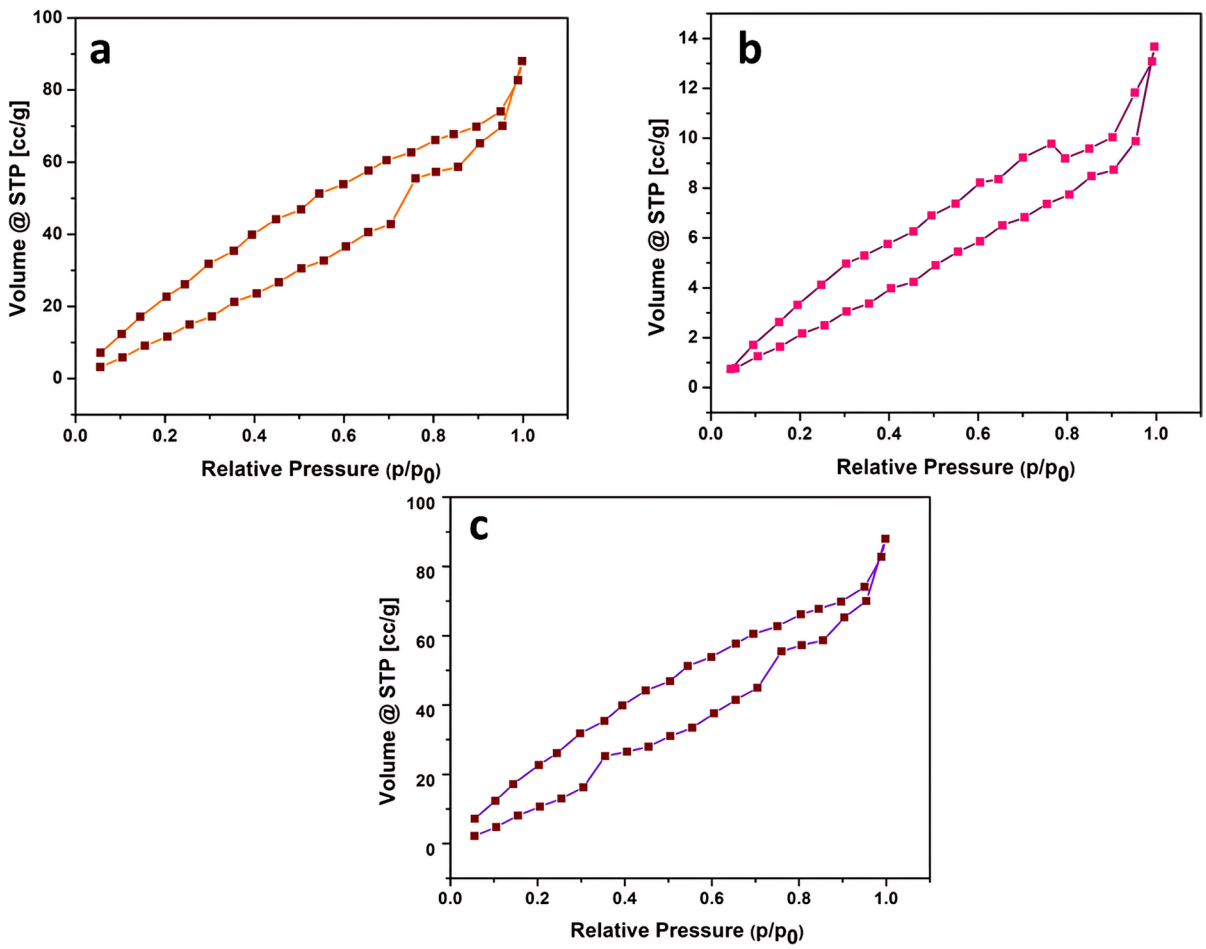

Fig. 8 N_2 adsorption-desorption isotherms of **a** raw bentonite, **b** surfactant-functionalized bentonite, and **c** silane-coupled bentonite

EGCG, the molecular motion resistance increased and the adsorption rate decreased gradually. The enhanced adsorption performance of functionalized clay may be due to the hydrophobic hydrogen and electrostatic interaction between the clay and EGCG (Xie et al., 2018). The functional groups of functionalized clay can strengthen the hydrogen-bonding interactions between modified

https://doi.org/10.1007/s42860-023-00246-4 Published online by Cambridge University Press

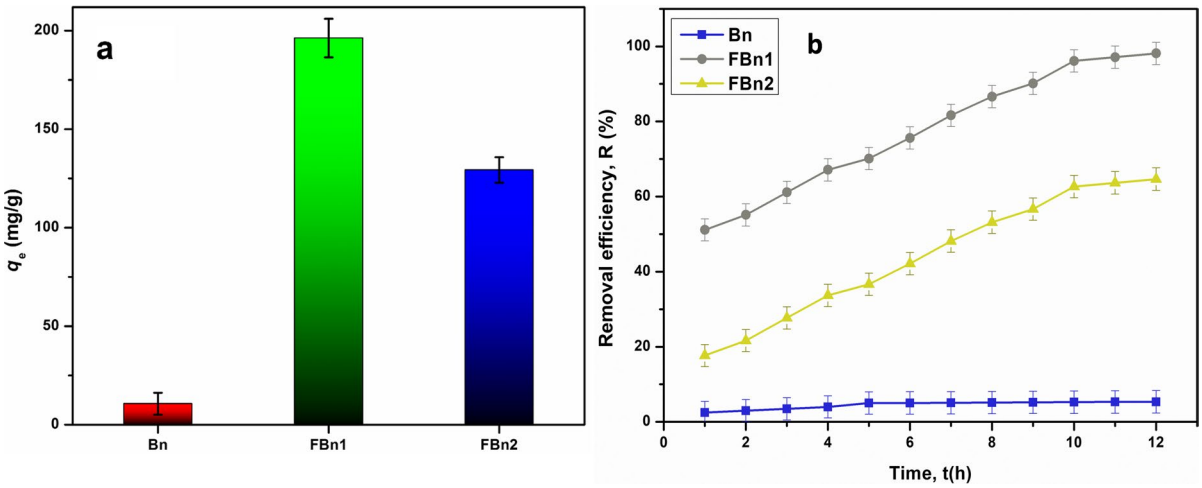

Fig. 9 **a** Amount of adsorption of EGCG and **b** removal efficiency of EGCG from raw bentonite, surfactant-functionalized bentonite, and silane-coupled bentonite

clay and the adsorbate (EGCG), which increases the adsorption affinity toward EGCG. The long hydrophobic alkyl chain provided a better adsorption rate for EGCG due to the intermolecular attraction between the hydroxyl group and positively polarized nitrogen of Aliquat 336, whereas interaction of EGCG with IBTS was relatively weak.

Adsorption Kinetics

The adsorption kinetics of the EGCG were studied on raw and functionalized clays. The value of the pseudo-first order adsorption rate constant, K_F, was determined by plotting the graph of $\log(q_e - q_t)$ vs. t. The adsorption isotherm of EGCG in an aqueous solution was a linear plot and shown in Fig. 10a. To optimize the adsorption system, it was essential to establish the adsorption kinetics and equilibrium (Baruah et al., 2015). Therefore, the adsorption equilibria from the Freundlich adsorption isotherm were interpreted. The adsorption density of EGCG as a function of time onto the raw, surfactant functionalized, and silane-functionalized clays is shown in Fig. 10b. The pseudo-first order and pseudo-second order plots for the adsorption of EGCG on raw, surfactant-functionalized, and silane-functionalized clay are shown in Fig. 10c and d.

Adsorption Mechanism

The clay surface has potential adsorption sites due to the presence of hydroxyl groups at their edges. The adsorption mechanism of EGCG on functionalized clay was interpreted through various interactions (Mahmoodi, 2013; Mahmoodi et al., 2010a, b, 2018) . The presence of Aliquat 336 within adjacent clay layers can interact electrostatically with EGCG through a positively charged nitrogen atom. In contrast, the oxygen of the methoxy group interacted through an n–π* interaction with the aromatic ring of EGCG. It generally involved the delocalization of the lone pair of O atoms into the π orbital of aromatic EGCG. The adsorption mechanism also included intermolecular hydrogen bonding in both cases. The availability of hydroxyl groups at the edges of the clay layers can mean H-bonding interactions with the –OH of EGCG. A diagrammatic representation of the adsorption mechanism is given in Fig. 11.

The surfactant and the silane-coupling agent both contain hydrophobic alkyl chains, whereas the surfactant Aliquat 336 contains long alkyl chain of C_8 and the isobutyl(trimethoxy)silane contains C_4 with branches. The greater exfoliation of stacked clay layers occurred in the clay-Aliquat 336 sample due to the long C_8 chain. So, more adsorption of polyphenol can be considered in clay-Aliquat 336 due to the greater exfoliation than that of clay-isobutyl(trimethoxy)silane.

https://doi.org/10.1007/s42860-023-00246-4 Published online by Cambridge University Press

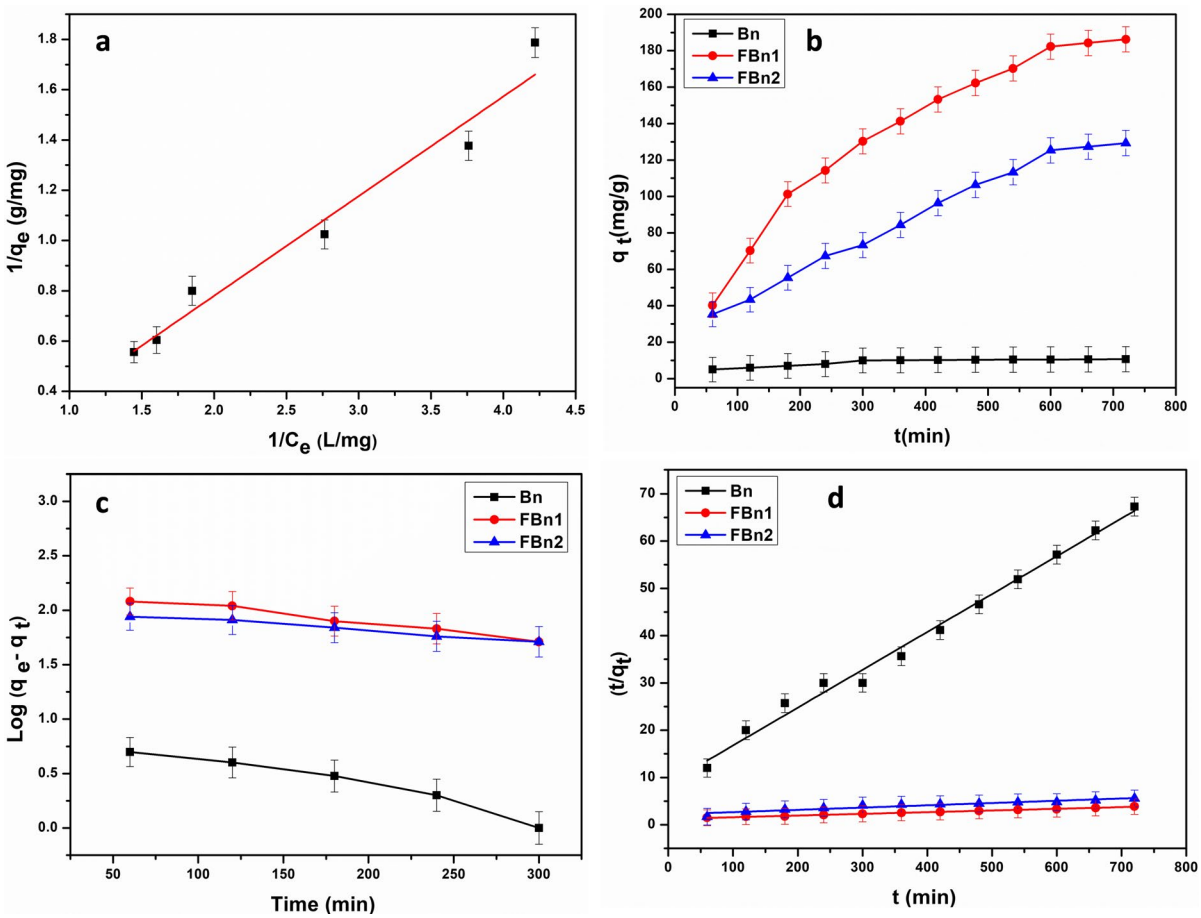

Fig. 10 **a** Freundlich adsorption isotherm for EGCG, **b** adsorption density as a function of time, **c** pseudo-first order plot, and **d** pseudo-second order plot for adsorption of EGCG on raw bentonite, surfactant-functionalized bentonite, and silane-coupled bentonite

values. EGCG acts as a weak acid in an aqueous solution, having a dissociation constant (pK_a) of 7.68 (Park et al. 2013). The effect of pH on the adsorption capacity of functionalized clay was investigated over the pH range of 3, 5, 7.5, 8, and 9 (Fig. 12). The adsorption increased with increasing pH, and the maximum adsorption observed was at pH 9. In case of silane-functionalized clay, the maximum adsorption was obtained as 120 mg/g. Both functionalized clays showed better adsorptive capacity of the EGCG in basic solutions. The continuous increase in adsorption of EGCG was observed in the case of Aliquat 336-modified clay, which showed the homogeneous increment corresponding to each pH value, and maximum adsorption was obtained at a pH of 9. In that case, the amount of EGCG adsorbed was 160 mg/g. The presence of organic filler in the interlayer space of bentonite acted as an efficient adsorbent for EGCG. The greater degree of adsorption in case of surfactant modified clay can be explained in terms of hydrophobic interaction and Van der Waals interaction. At high pH, the –OH groups available on the edge of the clay surface become deprotonated and, therefore, exhibit negative polarity. When the hydroxyl groups of EGCG come in contact with a basic environment, they also become deprotonated and undergo further stabilization through an aromatic ring current within the molecule. In addition to this, steric repulsion between negative polarities was also observed. Therefore, the adsorption of EGCG did not occur effectively for an acid-activated solution due to the predominant steric effect.

Interestingly, the functionalized clay intercalated with long hydrophobic alkyl chains laying adjacent to one another acted as an effective adsorbent. The increase in carbon content can contribute effectively

https://doi.org/10.1007/s42860-023-00246-4 Published online by Cambridge University Press

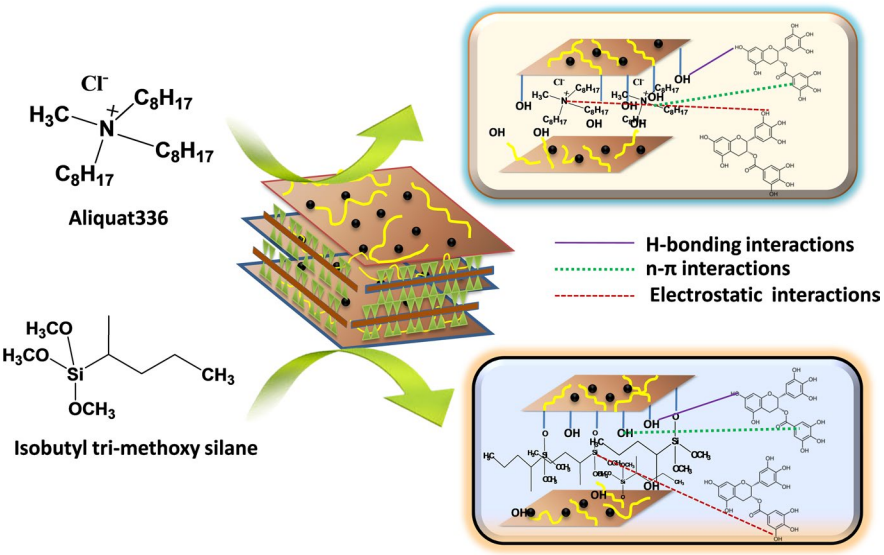

Fig. 11 Schematic diagram of adsorption of EGCG on functionalized clay, clay-Aliquat 336, and clay-IBTS

Studies of pH-dependent Adsorption of Epigallocatechin Gallate (EGCG)

The modified clays were used as adsorbents to study the pH-dependent adsorption of EGCG. The pH-dependent adsorption behavior of the organically modified clays showed that the amount adsorbed from 1 mg/L aqueous solution was estimated at 99% in 12 h (data not shown).

The polyphenols are highly sensitive under various pH environments (Hosseini et al., 2018), thus pH-dependent adsorption was studied at various pH to the lateral interaction of hydrophobic alkyl segments (Xie et al. 2018). No prominent adsorption of EGCG was observed (Fig. 9a) in the case of raw bentonite, its adsorption performance was, therefore, not studied in terms of pH.

Desorption and Regeneration Studies

The regeneration of adsorbent is necessary to make the adsorption process more economical (Hayati & Mahmoodi, 2012) and industrially feasible. The

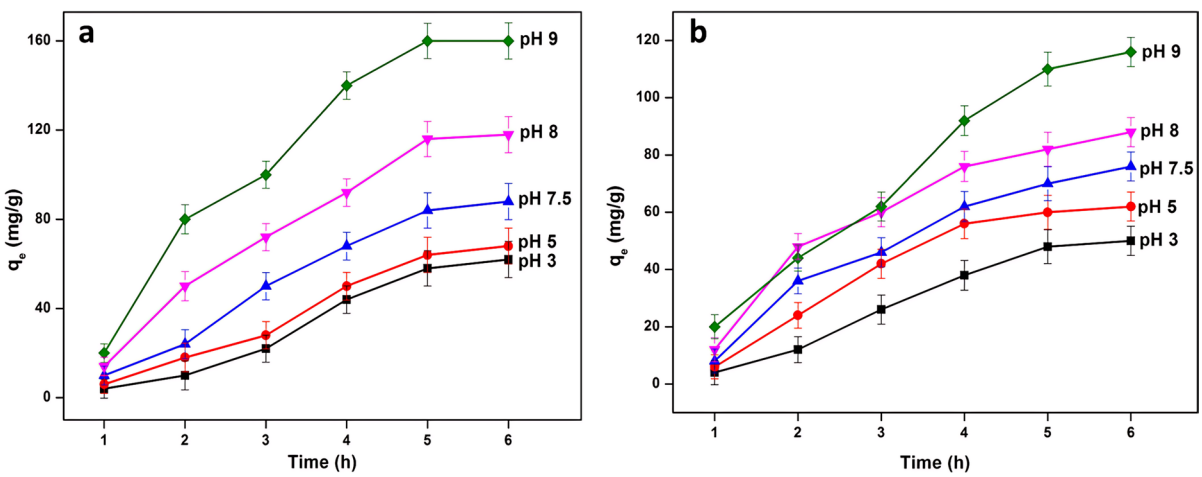

Fig. 12 Time-dependent adsorption of EGCG on functionalized clay **a** clay-Aliquat 336 and **b** clay-IBTS at various pH levels

https://doi.org/10.1007/s42860-023-00246-4 Published online by Cambridge University Press

Table 2 Adsorption–desorption of EGCG through four cycles

No of cycles	Adsorption (%)	Desorption (%)
1	95.4	94.3
2	91.56	91.42
3	89.31	86.52
4	87.08	84.13

pH-dependent adsorption experiments here revealed that further increases in pH above 9 causes EGCG adsorption to decrease, so this principle was exploited to desorb the EGCG from the adsorbate surface as a means to regenerate the adsorbent. NaOH solution was used in various concentrations (0.01, 0.05, 0.1, 0.5, and 1 M) to desorb the EGCG, and the respective concentrations gave desorption capacities of 74.3, 81.2, 90.5, 91.2, and 94.1%. The desorption of EGCG, thus, increased with increasing concentration of NaOH due to the formation of the sodium salt of EGCG, which could be removed easily. Desorption and regeneration experiments were performed with 0.1 M NaOH for four cycles and the percentage of adsorption and desorption is given in Table 2.

Conclusions

In the present study, organic modification of hydrophilic bentonite was studied using Aliquat 336 and isobutyl(trimethoxy)silane as modifying agents. The Aliquat 336 formed a reactive junction with bentonite through a nucleophilic substitution reaction at 1 atm pressure and ambient temperature. The modification of clay provided better intercalation of alkyl chains between the superimposed clay layers. The characterization of raw and functionalized clays revealed improved performance of surfactant-functionalized clay over raw bentonite. The surfactant functionalized clay acted as a good adsorbent for EGCG and adsorbed up to 196.26 mg/g, which was dependent on the pH of the medium. The kinetic data were analyzed using pseudo- first order and pseudo-second order models.

Acknowledgements The authors acknowledge CSIR New Delhi for financial support under MLP 1018 and the Director of CSIR-NEIST for his keen interest in the subject and for encouraging the research group.

Funding Funding sources are as stated in the Acknowledgments.

Data Availability Data available upon reasonable request.

Declarations

Conflict of Interest The authors declare that they have no conflict of interest.

References

Abeywardena, S. B., Perera, S., Nalin de Silva, K. M., & Tissera, N. P. (2017). A facile method to modify bentonite nanoclay with silane. *International Nano Letters, 7*(3), 237–241. https://doi.org/10.1007/s40089-017-0214-2

Anastácio, A. S., Aouad, A., Sellin, P., Fabris, J. D., Bergaya, F., & Stucki, J. W. (2008). Characterization of a redox-modified clay mineral with respect to its suitability as a barrier in radioactive waste confinement. *Applied Clay Science, 39*(3–4), 172–179. https://doi.org/10.1016/j.clay.2007.05.007

Anirudhan, T. S., & Ramachandran, M. (2015). Adsorptive removal of basic dyes from aqueous solutions by surfactant modified bentonite clay (functionalized clay): Kinetic and competitive adsorption isotherm. *Process Safety and Environmental Protection, 95*, 215–225. https://doi.org/10.1016/j.psep.2015.03.003

Asefi, D., Arami, M., Sarabi, A. A., & Mahmoodi, N. M. (2009). The chain length influence of cationic surfactant and role of nonionic co-surfactants on controlling the corrosion rate of steel in acidic media. *Corrosion Science, 51*(8), 1817–1821. https://doi.org/10.1016/j.corsci.2009.05.007

Asefi, D., Mahmoodi, N. M., & Arami, M. (2010). Effect of nonionic co-surfactants on corrosion inhibition effect of cationic gemini surfactant. *Colloids and Surfaces a: Physicochemical and Engineering Aspects, 355*(1–3), 183–186. https://doi.org/10.1016/j.colsurfa.2009.12.019

Avella, M., Cosco, S., Volpe, G. D., & Errico, M. E. (2005). Crystallization behavior and properties of exfoliated isotactic polypropylene/functionalized clay nanocomposites. *Advances in Polymer Technology: Journal of the Polymer Processing Institute, 24*(2), 132–144. https://doi.org/10.1002/ADV.20036

Bai, H., Zhao, Y., Wang, W., Zhang, T., Yi, H., & Song, S. (2019). Effect of interlayer cations on exfoliating 2D montmorillonite nanosheets with high aspect ratio: From experiment to molecular calculation. *Ceramics International, 45*(14), 17054–17063. https://doi.org/10.1016/j.ceramint.2019.05.257

Baruah, K., Bhattacharyya, P. K., & Hazarika, S. (2015). Adsorption of dilute alcohols onto cyclodextrin–polysulfone membrane: Experimental and theoretical analysis. *Journal of Chemical & Engineering Data, 60*(9), 2549–2558. https://doi.org/10.1021/acs.jced.0c00234

Beltrán, M. I., Benavente, V., Marchante, V., Dema, H., & Marcilla, A. (2014). Characterisation of montmorillonites simultaneously modified with an organic dye and an ammonium salt at different dye/salt ratios. Properties of these modified montmorillonites EVA nanocomposites.

Applied Clay Science, 97, 43–52. https://doi.org/10.1016/j.clay.2014.06.001

Bergaya, F., & Lagaly, G. (2006). General introduction: Clays, clay minerals, and clay science. *Developments in Clay Science, 1*, 1–18. https://doi.org/10.1016/S1572-4352(05)01001-9

Borah, A., Gogoi, M., Goswami, R., Sarmah, H., Hazarika, K. K., & Hazarika, S. (2022). Thin film nanocomposite membrane incorporated with clay-ionic liquid framework for enhancing rejection of epigallocatechin gallate in aqueous media. *Journal of Environmental Chemical Engineering, 10*(3), 107423. https://doi.org/10.1016/j.jece.2022.107423

Chanra, J., Budianto, E., & Soegijono, B. (2019, April). Surface modification of montmorillonite by the use of organic cations via conventional ion exchange method. In *IOP Conference Series: Materials Science and Engineering* (Vol. 509, No. 1, p. 012057). IOP Publishing. https://doi.org/10.1088/1757-899X/509/1/012057

Chiu, C. W., Huang, T. K., Wang, Y. C., Alamani, B. G., & Lin, J. J. (2014). Intercalation strategies in clay/polymer hybrids. *Progress in Polymer Science, 39*(3), 443–485. https://doi.org/10.1016/j.progpolymsci.2013.07.002

De Paiva, L. B., Morales, A. R., & Díaz, F. R. V. (2008). Organoclays: Properties, preparation and applications. *Applied Clay Science, 42*(1–2), 8–24. https://doi.org/10.1016/j.clay.2008.02.006

Düşkünkorur, H. Ö., Bégué, A., Pollet, E., Phalip, V., Güvenilir, Y., & Avérous, L. (2015). Enzymatic ring-opening (co) polymerization of lactide stereoisomers catalyzed by lipases. Toward the insitu synthesis of organic/inorganic nanohybrids. *Journal of Molecular Catalysis b: Enzymatic, 115*, 20–28. https://doi.org/10.1016/J.MOLCATB.2015.01.011

Guo, F., Aryana, S., Han, Y., & Jiao, Y. (2018). A review of the synthesis and applications of polymer–nanoclay composites. *Applied Sciences, 8*(9), 1696. https://doi.org/10.3390/app8091696

Hayati, B., & Mahmoodi, N. M. (2012). Modification of activated carbon by the alkaline treatment to remove the dyes from wastewater: Mechanism, isotherm and kinetic. *Desalination and Water Treatment, 47*(1–3), 322–333. https://doi.org/10.1080/19443994.2012.696429

He, H., Frost, R. L., Bostrom, T., Yuan, P., Duong, L., Yang, D., & Kloprogge, J. T. (2006). Changes in the morphology of organoclays with HDTMA+ surfactant loading. *Applied Clay Science, 31*(3–4), 262–271. https://doi.org/10.1016/j.clay.2005.10.011

Hosseini, S. A., Vossoughi, M., Mahmoodi, N. M., & Sadrzadeh, M. (2018). Efficient dye removal from aqueous solution by high-performance electrospun nanofibrous membranes through incorporation of SiO_2 nanoparticles. *Journal of Cleaner Production, 183*, 1197–1206. https://doi.org/10.1016/j.jclepro.2018.02.168

Kim, N. H., Malhotra, S. V., & Xanthos, M. (2006). Modification of cationic nanoclays with ionic liquids. *Microporous and Mesoporous Materials, 96*(1–3), 29–35. https://doi.org/10.1016/j.micromeso.2006.06.017

Komori, Y., Sugahara, Y., & Kuroda, K. (1999). Intercalation of alkylamines and water into kaolinite with methanol kaolinite as an intermediate. *Applied Clay Science, 15*(1–2), 241–252. https://doi.org/10.1016/S0169-1317(99)00014-9

Kozak, M., & Domka, L. (2004). Adsorption of the quaternary ammonium salts on montmorillonite. *Journal of Physics and Chemistry of Solids, 65*(2–3), 441–445. https://doi.org/10.1016/j.jpcs.2003.09.015

Leung, S. Y., Lam, D. C. C., & Wong, C. P. (2001). Experimental investigation of time dependent degradation of coupling agent bonded interfaces. In: *2001 Proceedings. 51st Electronic Components and Technology Conference (Cat. No. 01CH37220)* (pp. 1333–1337). IEEE. https://doi.org/10.1109/ECTC.2001.928004

Li, P., Khan, M. A., Xia, M., Lei, W., Zhu, S., & Wang, F. (2019). Efficient preparation and molecular dynamic (MD) simulations of Gemini surfactant modified layered montmorillonite to potentially remove emerging organic contaminants from wastewater. *Ceramics International, 45*(8), 10782–10791. https://doi.org/10.1016/j.ceramint.2019.02.152

Li, Y., Hu, X., Liu, X., Zhang, Y., Zhao, Q., Ning, P., & Tian, S. (2018). Adsorption behavior of phenol by reversible surfactant-modified montmorillonite: Mechanism, thermodynamics, and regeneration. *Chemical Engineering Journal, 334*, 1214–1221. https://doi.org/10.1016/j.cej.2017.09.140

Mahmoodi, N. M. (2013). Nickel ferrite nanoparticle: Synthesis, modification by surfactant and dye removal ability. *Water, Air, & Soil Pollution, 224*(2), 1–11. https://doi.org/10.1007/s11270-012-1419-7

Mahmoodi, N. M., & Arami, M. (2009). Numerical finite volume modelling of dye decolorization using immobilized titania nano-photocatalysis. *Chemical Engineering Journal, 146*(2), 189–193. https://doi.org/10.1016/j.cej.2008.05.036

Mahmoodi, N. M., Hayati, B., & Arami, M. (2010a). Textile dye removal from single and ternary systems using date stones: Kinetic, isotherm, and thermodynamic studies. *Journal of Chemical & Engineering Data, 55*(11), 4638–4649. https://doi.org/10.1021/je1002384

Mahmoodi, N. M., Hayati, B., Arami, M., & Mazaheri, F. (2010b). Single and binary system dye removal from colored textile wastewater by a dendrimer as a polymeric nanoarchitecture: Equilibrium and kinetics. *Journal of Chemical & Engineering Data, 55*(11), 4660–4668. https://doi.org/10.1021/je100248m

Mahmoodi, N. M., Arami, M., Bahrami, H., & Khorramfar, S. (2010c). Novel biosorbent (Canola hull): Surface characterization and dye removal ability at various cationic dye concentrations. *Desalination, 264*(1–2), 134–142. https://doi.org/10.1016/j.desal.2010.07.017

Mahmoodi, N. M., Taghizadeh, M., & Taghizadeh, A. (2018). Mesoporous activated carbons of low-cost agricultural bio-wastes with high adsorption capacity: Preparation and artificial neural network modelling of dye removal from single and multicomponent (binary and ternary) systems. *Journal of Molecular Liquids, 269*, 217–228. https://doi.org/10.1016/j.molliq.2018.07.108

Manias, E., Touny, A., Wu, L., Strawhecker, K., Lu, B., & Chung, T. C. (2001). Polypropylene/montmorillonite nanocomposites. Review of the synthetic routes and materials properties. *Chemistry of Materials, 13*(10), 3516–3523. https://doi.org/10.1021/cm0110627

Moreno, M., Benavente, E., González, G., Lavayen, V., & Torres, C. M. S. (2006). Functionalization of bentonite by intercalation of surfactants. *Molecular Crystals and Liquid Crystals*, *448(1)*, 123–725. https://repositorio.uchile.cl/handle/2250/118840

Moshe, S. B., & Rytwo, G. (2018). Thiamine-based functionalized clay for phenol removal from water. *Applied Clay Science, 155*, 50–56. https://doi.org/10.1016/j.clay.2018.01.003

Naranjo, P. M., Sham, E. L., Castellon, E. R., Torres Sánchez, M., & Farfan Torres, E. M. (2013). Identification and quantification of the interaction mechanisms between the cationic surfactant HDTMA-Br and montmorillonite. *Clays and Clay Minerals, 61*(2), 98–106. https://doi.org/10.1346/CCMN.2013.0610208

Ouellet-Plamondon, C. M., Stasiak, J., & Al-Tabbaa, A. (2014). The effect of cationic, non-ionic and amphiphilic surfactants on the intercalation of bentonite. *Colloids and Surfaces a: Physicochemical and Engineering Aspects, 444*, 330–337. https://doi.org/10.1016/j.colsurfa.2013.12.032

Oveisi, M., Mahmoodi, N. M., & Asli, M. A. (2019). Facile and green synthesis of metal-organic framework/inorganic nanofiber using electrospinning for recyclable visible-light photo catalysis. *Journal of Cleaner Production, 222*, 669–684. https://doi.org/10.1016/j.jclepro.2019.03.066

Oyanedel-Craver, V. A., Fuller, M., & Smith, J. A. (2007). Simultaneous sorption of benzene and heavy metals onto two organoclays. *Journal of Colloid and Interface Science, 309*(2), 485–492. https://doi.org/10.1016/j.jcis.2006.10.001

Ozturk, H., Pollet, E., Phalip, V., Guvenilir, Y., & Averous, L. (2016). Nanoclays for lipase immobilization: Biocatalyst characterization and activity in polyester synthesis. *Polymers, 8*(12), 416. https://doi.org/10.3390/polym8120416

Pandey, P., & De, N. (2018). Surfactant-induced changes in physicochemical characters of bentonite clay. *International Research Journal of Pure and Applied Chemistry, 15*(4), 1–11. https://doi.org/10.9734/IRJPAC/2017/39374

Park, Y., Ayoko, G. A., & Frost, R. L. (2011). Application of organoclays for the adsorption of recalcitrant organic molecules from aqueous media. *Journal of Colloid and Interface Science, 354*(1), 292–305. https://doi.org/10.1016/j.jcis.2010.09.068

Park, Y., Ayoko, G. A., Kurdi, R., Horváth, E., Kristóf, J., & Frost, R. L. (2013). Adsorption of phenolic compounds by functionalized clays: Implications for the removal of organic pollutants from aqueous media. *Journal of Colloid and Interface Science, 406*, 196–208. https://doi.org/10.1016/j.jcis.2013.05.027

Pernyeszi, T., Kasteel, R., Witthuhn, B., Klahre, P., Vereecken, H., & Klumpp, E. (2006). Functionalized clay for soil remediation: Adsorption of 2, 4-dichlorophenol on functionalized clay/aquifer material mixtures studied under static and flow conditions. *Applied Clay Science, 32*(3–4), 179–189. https://doi.org/10.1016/j.colsurfa.2004.11.049

Raji, M., Mekhzoum, M. E. M., Rodrigue, D., & Bouhfid, R. (2018). Effect of silane functionalization on properties of polypropylene/clay nanocomposites. *Composites Part B: Engineering, 146*, 106–115. https://doi.org/10.1016/j.compositesb.2018.04.013

Terzic, A., Pezo, L., Andric, L., Pavlović, V. B., & Mitic, V. V. (2017). Optimization of bentonite clay mechanochemical activation using artificial neural network modelling. *Ceramics International, 43*(2), 2549–2562. https://doi.org/10.1016/j.ceramint.2016.11.058

Tian, Q., Qi, Y., Qin, S., Wu, F., Long, L., Xu, G., & Yin, X. (2017). Effect of Surfactant Concentration on Thermal and Mechanical Properties of Poly (Butylene Succinate)/Functionalized clay Composites. *Journal of Macromolecular Science, Part B, 56*(7), 474–492. https://doi.org/10.1080/00222348.2017.1327298

Tonle, I. K., Ngameni, E., Tchieno, F. M., & Walcarius, A. (2015). Functionalized clay-modified electrodes: Preparation, characterization and recent electroanalytical applications. *Journal of Solid State Electrochemistry, 19*(7), 1949–1973. https://doi.org/10.1007/s10008-014-2728-0

Xie, S., Wen, Z., Zhan, H., & Jin, M. (2018). An experimental study on the adsorption and desorption of Cu (II) in silty clay. *Geofluids, 2018*, 3610921. https://doi.org/10.1155/2018/3610921

Zampori, L., Stampino, P. G., Cristiani, C., Dotelli, G., & Cazzola, P. (2010). Synthesis of functionalized clays using non-ionic surfactants: Effect of time, temperature and concentration. *Applied Clay Science, 48*(1–2), 97–102. https://doi.org/10.1016/j.clay.2009.11.015

Zhang, C., Cui, F., Zeng, G. M., Jiang, M., Yang, Z. Z., Yu, Z. G., & Shen, L. Q. (2015). Quaternary ammonium compounds (QACs): A review on occurrence, fate and toxicity in the environment. *Science of the Total Environment, 518*, 352–362. https://doi.org/10.1016/j.scitotenv.2015.03.007

Zhou, Q., Zhu, R., Parker, S. C., Zhu, J., He, H., & Molinari, M. (2015). Modelling the effects of surfactant loading level on the sorption of organic contaminants on functionalized clays. *RSC Advances, 5*(58), 47022–47030. https://doi.org/10.1039/C5RA05998D

Zumsteg, R., Plötze, M., & Puzrin, A. (2014). Reduction of the clogging potential of clays: new chemical applications and novel quantification approaches. In: *Bio-and Chemo-Mechanical Processes in Geotechnical Engineering: Géotechnique Symposium in Print 2013* (pp. 44–54). ICE Publishing. https://doi.org/10.1680/geot.SIP13.P.005